Characterization of Tape Edge Contact Force With Acoustic Emission

Bart Raeymaekers

Frank E. Talke

University of California, San Diego,
Center for Magnetic Recording Research,
9500 Gilman Drive, #0401,
La Jolla, CA 92093

Acoustic emission sensors were used to detect contact between a moving tape and the flange of a tape guide. The influence of tape drive operating conditions on the tape edge contact force was studied. A one-dimensional model was developed to predict the magnitude of tape/flange impact. The model fits the experimental data well. [DOI: 10.1115/1.2748775]

1 Introduction

Lateral tape motion (LTM) is defined as the time-dependent displacement of magnetic tape perpendicular to the tape transport direction. The main sources of lateral tape motion are run-out of tape reels and tape rollers, tape tension transients, staggered wraps (stack-shifts) in the supply reel, and contact between the tape edge and a flange (roller or reel). A servo loop controls the magnetic read/write head actuator and compensates the lateral displacement of the tape up to a limited bandwidth. LTM with a frequency higher than the bandwidth of the servo actuator (typically >1 kHz) is generally referred to as high frequency LTM and can cause track misregistration between the read/write head and a previously written track. Hence, LTM limits the track (recording) density [1] and must be decreased to accommodate a narrower track width for future high performance tape drives [2].

Researchers in the past have investigated various aspects related to tape/edge contact [3–9]. However, little published information exists regarding the magnitude of contact forces during tape edge/flange contact. Since tape edge wear and LTM are related to the magnitude of the tape edge contact force [4,9], this information would be desirable for the design of future high performance tape drives. This paper tries to fill the above gap and focuses on the characterization and quantification of tape edge contact between a tape edge and the flange of a roller by means of acoustic emission (AE) techniques.

2 Acoustic Emission

In this investigation, an acoustic emission (AE) sensor [10,11] is used as a flange instead of an actual flange on a roller. When the tape makes contact with the flange, which is replaced by the sensor, a voltage is generated. This voltage is analyzed and used as an indicator of the type and strength of contact occurring as a function of tape drive operating parameters.

3 Calibration

To determine the magnitude of the contact force between the tape edge and a flange, the AE sensor was first calibrated by means of the "ball drop method" [12]. This method has previously been used for the analysis of slider/disk impacts in hard disk drive research [13,14]. Figure 1 illustrates the calibration procedure. A steel ball is dropped from different heights h on a load cell that measures the impact force during contact (Fig. 1(a)). Next, a steel ball is dropped on the AE sensor and the maximum output voltage is measured (Fig. 1(b)). To insure that the impact of the steel ball occurs at the same position for all experiments, a small tube has been used to guide the ball. Correlating the load cell (force) data and the AE (voltage) data, the relationship between AE voltage and impact force was established and shown in Fig. 1(c). The calibration experiment was repeated five times and the results were averaged over all repetitions. The ball drop calibration method must be interpreted with care since the impact of a steel ball on an AE transducer results in a different contact situation from that of a tape edge and an AE transducer. Therefore, the ball drop calibration gives only an estimate of the impact force, rather than an exact value.

4 Detection of Tape/Flange Contact

Figure 2 shows the experimental setup used to study contact between a tape and the flange of a roller.

Magnetic tape from the supply reel is guided over a smooth roller with only a bottom flange, before being wound on the take-up reel. The wrap angle θ was set to be 60 deg. The AE sensor is positioned above the roller and acts as an "artificial flange." An LTM edge sensor [1] is positioned over the tape to measure LTM.

Figure 3(a) shows the measured LTM signal versus time. Figure 3(b) shows the LTM signal versus time, after high-pass filtering at 1 kHz while Fig. 3(c) shows the root mean square (rms) impact force between the tape and the flange, also as a function of time. The rms impact force is derived from the rms AE voltage and is thus related to the energy content of the AE signal [11]. Figure 3(d) depicts the time frequency analysis of the LTM. In the time frequency analysis, a darker color denotes a higher magnitude for a particular frequency component.

Figure 3 reveals that high frequency LTM bursts (Fig. 3(b)) occur at the same time when impact occurs between the tape and a flange denoted by the peaks in the rms impact force (Fig. 3(c)). It is thus apparent that contact between tape and roller flange causes high frequency LTM, as emphasized by the three vertical dashed lines. Note that the rms impact force never reaches zero, due to background noise in the AE measurement. Furthermore, Fig. 3(d) reveals that the high frequency components of the LTM, caused by tape edge contact, predominantly occur in the 1–2 kHz range. Since the servo actuator can track LTM up to a bandwidth of approximately 1 kHz, the LTM components with a frequency below 1 kHz are less important.

After establishing the usefulness of AE probes in monitoring tape edge contact, the influence of the tape speed, the tape tension, and the supply pack diameter (whether the reel is full or empty) on tape/flange contact was investigated. Figure 4 shows the average impact force versus the diameter of the supply reel tape pack (position). The background noise level for a stationary tape is indicated by the dotted line.

The impact force was averaged over one second of data. Hence, the magnitude as well as the frequency of the impacts is taken into account. It is observed that the average impact force reaches a maximum when the tape reel diameter is halfway between an empty and a full tape reel. Figure 4 also indicates that the impact force increases with increasing tape speed and decreasing tape tension.

A tape reel is misaligned due to manufacturing and assembly tolerances for a given azimuth angle α. Therefore, the tape is leaving the rotating reel with a periodic lateral displacement. The amplitude of this lateral displacement A depends on the diameter D (position) of the tape pack on the supply reel and the azimuth angle α, and can be expressed as

Contributed by the Technical Committee on Vibration and Sound of ASME for publication in the JOURNAL OF VIBRATION AND ACOUSTICS. Manuscript received June 10, 2006; final manuscript received April 4, 2007. Associ. Editor: Jonathan A. Wickert.

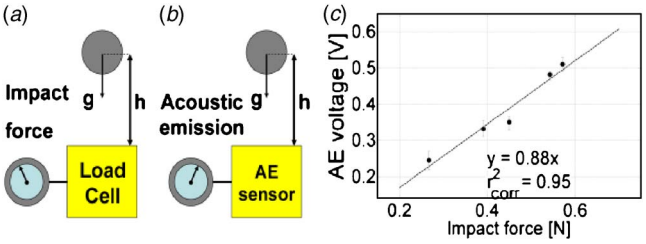

Fig. 1 "Ball drop method" calibration procedure

$$A = \left(\frac{D\alpha}{2}\right)\cos\left(\frac{2Vt}{D}\right) \tag{1}$$

where V represents the constant linear tape speed and t represents the time. A full pack (outer diameter) causes the largest lateral displacement, while an empty pack (inner diameter) causes the smallest lateral displacement. In practice, the amplitude of the lateral displacement could be slightly different than the linear relationship $D\alpha/2$, due to the effect of stress created by a tensioned tape pack (see Fig. 6). However, the simplified expression in Eq. (1) is sufficient to explain the effect of the changing pack diameter on the amplitude and the frequency of the run-out. To keep the tape speed constant, it is necessary that the rotational frequency $\omega_r = 2V/D$ of the tape reel is changed continuously while the pack changes its size. Thus, the frequency of impact between the tape edge and a roller flange increases for a decreasing pack size, since the rotational speed of the decreasing pack size must increase. The effect of the increasing lateral displacement amplitude A versus decreasing rotational frequency ω_r for increasing pack diameter D oppose each other with respect to the magnitude of the impact force. For an increasing pack diameter, the magnitude of the impact force will increase, while its frequency of occurrence decreases. Averaging the impact force over a certain time span (1 s in Fig. 4) results in a maximum of the contact force at the middle diameter of the tape reel.

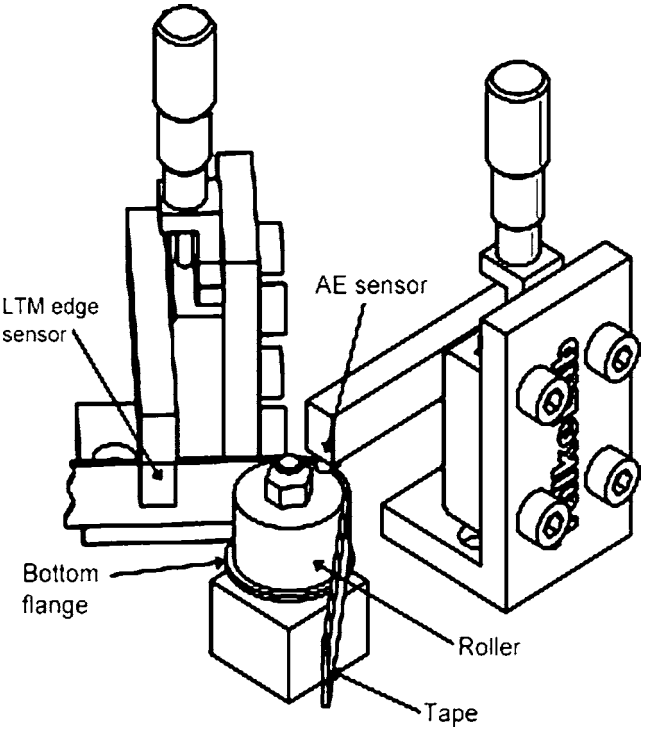

Fig. 2 Experimental setup

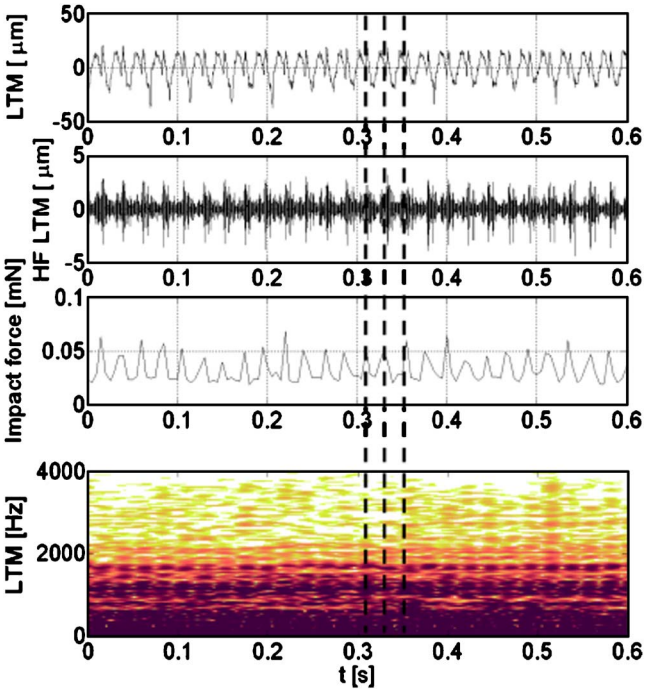

Fig. 3 (*a*) LTM, (*b*) 1 kHz high pass filtered LTM, (*c*) rms impact force, versus time, and d) time frequency analysis of LTM

5 Impact Between Tape Edge and Flange

The tape/flange impact can be modeled as a forced, single degree of freedom, mass spring system with "dry" friction. Since the direction of the friction force is always opposite to the direction of motion, the friction force is a piecewise constant function with respect to time. Fundamental research on so-called "impact oscillators" has been performed by several researchers [15–17]. Figure 5(*a*) shows the physical system of a tape sliding over a roller while Fig. 5(*b*) illustrates the mathematical model used to simulate the physical system.

A point mass, representing the tape, is connected with a spring to a fixed base and slides over the surface that represents the roller, thereby creating a piecewise constant friction force F_f, opposite to the direction of the lateral tape motion dx/dt. The spring (effective tape stiffness k) introduces a force F_s. Furthermore the

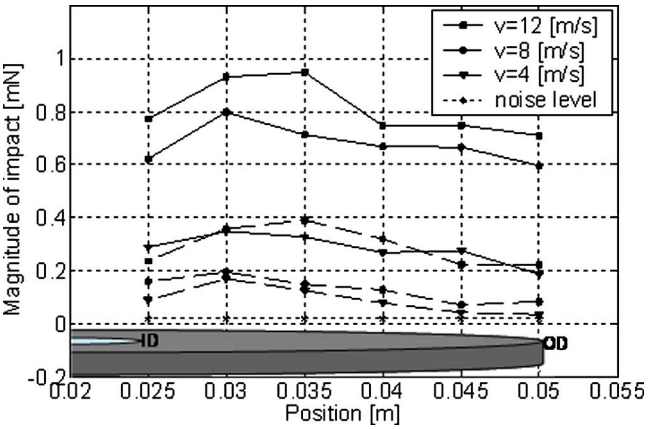

Fig. 4 Experimentally measured average impact force versus supply reel tape pack size, for a nominal tape tension of 1 N (solid lines) and 2 N (dashed lines) and for different tape speeds

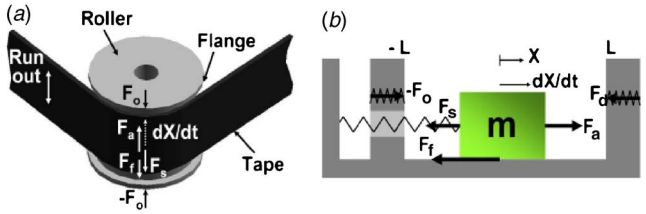

Fig. 5 (*a*) Physical model and (*b*) mathematical model

mass m is actuated by a harmonic force F_a, representing the reel run-out that forces the tape to move up and down when coming off the supply pack. Both flanges of the roller are represented by springs with a stiffness k_0, which is several orders of magnitude higher than the effective tape stiffness k. These springs come into play when the tape edge (point mass) reaches the position L of the flange and they require a large force F_0 to be compressed, i.e., the springs simulate an impact. When the tape edge does not touch a flange, the spring k_0 is not present in the model. It is assumed that tape buckling does not occur in our model.

Hence, the equation of motion is given by

$$m\frac{d^2x}{dt^2} + kx + \mu N \operatorname{sign}\left(\frac{dx}{dt}\right) = F_a \cos \omega_r t - k_0 \mathrm{H}(x^2 - L^2)(x - L) \tag{2}$$

where x represents the position of the tape on the roller and L represents the position of the flanges. Since the tape of finite width w is represented as a point mass, L represents the clearance between the tape edge and the flanges. Furthermore, $k = m\omega_n^2$ is the effective stiffness of the tape (lateral bending stiffness). The natural frequency of the tape is ω_n and m represents the tape mass. The friction coefficient is μ and N is the normal force acting on the tape. F_a is the amplitude and ω_r is the frequency of the applied harmonic force while t represents the time. H is the Heaviside function and introduces the spring with stiffness k_0 and corresponding force F_0 in the model, when the tape edge touches a flange.

Nondimensionalization of Eq. (2) with $X = x/L$, $\Lambda = t\omega_n$, $F = F_a/(mL\omega_n^2) = F_a/(kL)$, and $K = k_0/k$ yields

$$\frac{d^2X}{d\Lambda^2} + X + \operatorname{sign}\left(\frac{dX}{d\Lambda}\right)\frac{\mu N}{kL} = F \cos\left(\frac{\omega_r}{\omega_n}\right)\Lambda - KH(X^2 - 1)(X - 1) \tag{3}$$

In Eq. (3), the linear tape transport speed enters the model through the rotational frequency ω_r of the supply reel. Since $\omega_n = \sqrt{k/m}$, the effective stiffness k has to be determined.

When the tape is considered an elastic beam of length l (Euler-Bernoulli), centrally loaded with a point force P, the ratio of the applied force to the maximum deflection can be found as [18]

$$\frac{P}{d_{\max}} = \frac{48EI}{l^3} = k \tag{4}$$

where E represents the Young's modulus and I denotes the moment of inertia of the cross section of the tape. The belt-wrap force N, of the tape around the guide as a result of the tension T in the tape is given by

$$N = 2T \sin(\theta/2) \tag{5}$$

The axial run-out at a certain tape pack diameter is simulated by the harmonic force applied on the tape (mass). The axial run-out of the supply reel was measured with a dial indicator at different radial positions for the corresponding supply pack diameters, i.e., the pack diameter was adjusted to a desired radial position and the axial run-out at that position was measured. The results for the axial run-out versus radial position (pack diameter) are presented in Fig. 6.

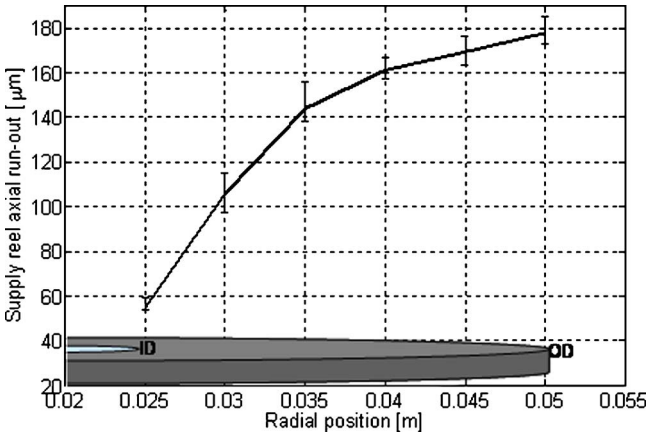

Fig. 6 Axial run-out of supply reel for different pack diameters

Figure 6 shows that the axial run-out increases with increasing pack diameter (radial position), from about 60 μm at the inner diameter to almost 180 μm at the outer diameter. In our simulation, the harmonic forcing function F_a was calculated as the product of the measured run-out and the effective tape stiffness k. The following parameters were used: tape width $w = 0.0127$ m, tape thickness $= 9$ μm, length $l = 0.01$ m, and Young's modulus and density of magnetic tape (PET substrate) $E = 7$ GPa and $\rho = 1370$ kg/m^3, respectively. The ratio of the flange stiffness versus the tape stiffness, $K = k_0/k$, was chosen to be 10^4. The position of the flange $L = 0.001$ m and the wrap angle $\theta = 60$ deg. Assuming a typical friction coefficient of $\mu = 0.2$ [19,20] and using the fourth order Runge Kutta method, we solved Eq. (3) for the following initial conditions:

$$X = 0.95 \tag{6}$$

$$\frac{dX}{d\Lambda} = 0 \tag{7}$$

Figure 7 shows the simulation results for the average impact force, calculated from the simulated $F_0(t)$, averaged over 1 s.

The one-dimensional model is only a crude approximation of the real phenomenon, which is three-dimensional. Although the

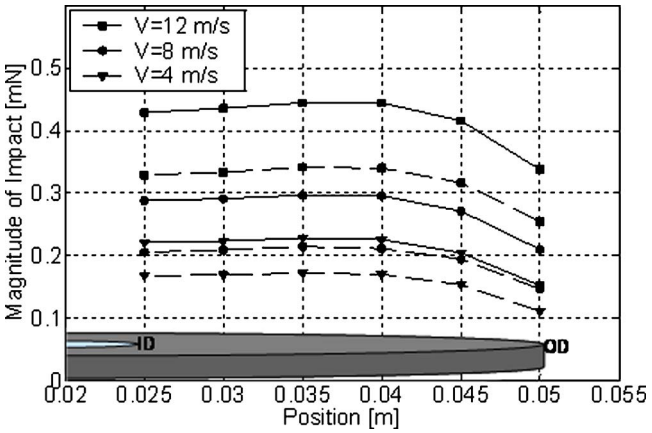

Fig. 7 Simulated average impact force versus supply reel tape pack size, for a nominal tape tension of 1 N (solid lines) and 2 N (dashed lines) and for different tape speeds

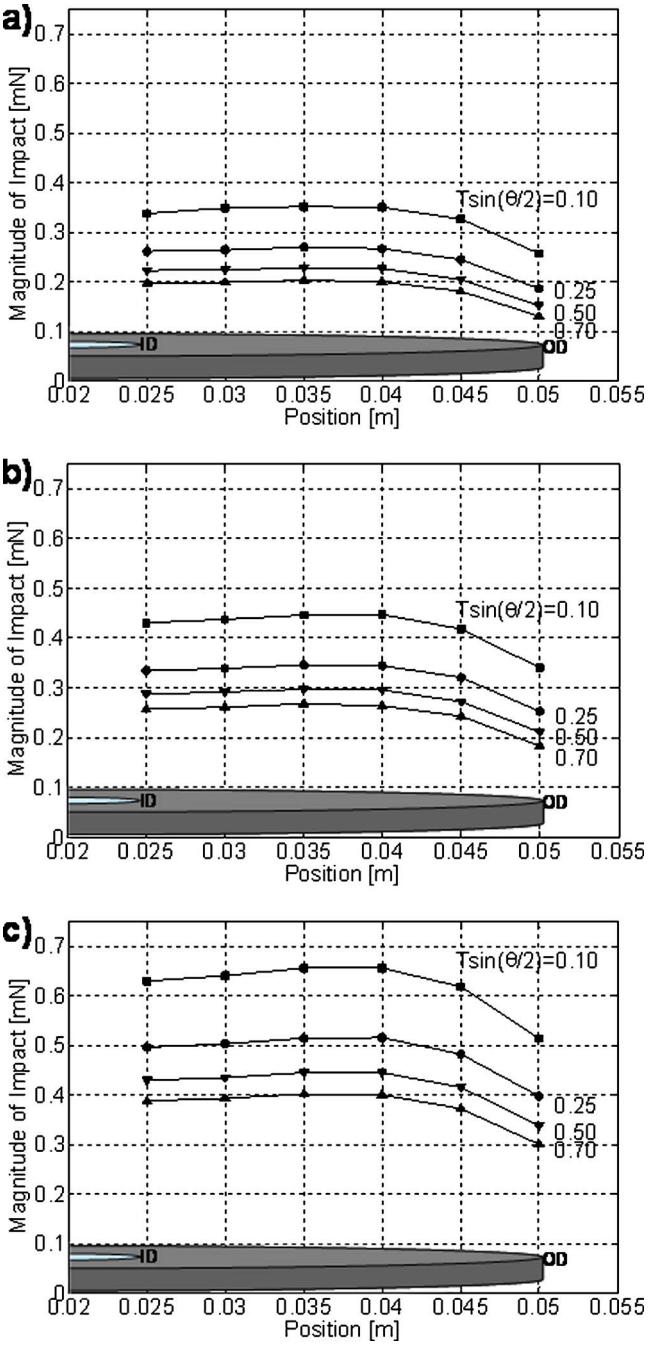

Fig. 8 Simulated average impact force versus supply reel tape pack size, for different values of $T\sin(\theta/2)$ and for a tape speed of (*a*) 4 m/s, (*b*) 8 m/s, and (*c*) 12 m/s

numerical values are not exactly matching the experimentally measured results, they are on the same order of magnitude and the simplified model captures the trends well.

Figure 8 shows the effect of tape speed, tape tension, and wrap angle on the magnitude of the tape/flange impact with respect to the pack radius (position). Since the tension as well as the wrap angle enter the model through the normal force N (see Eq. (5)), their effect can be evaluated by investigating the effect of $T\sin(\theta/2)$ on the magnitude of the average impact force.

Increasing $T\sin(\theta/2)$ reduces the impact force between roller flange and tape. In addition, Fig. 8 reveals that regardless of the tape speed, the impact for $T\sin(\theta/2)=0.1$ is almost double the value for $T\sin(\theta/2)=0.7$. This result is especially interesting when considering reduced nominal tape tension to accommodate thinner tapes. On the other hand, increasing the wrap angle decreases the average impact force, but also increases the contact surface between tape and roller and the friction that acts on the tape will increase accordingly. Friction will dissipate energy and hence, the average magnitude of the impact between tape and flange will be smaller. Figure 8 also illustrates that increasing tape speed increases the average magnitude of the impact. However, the effect of speed appears to be less than the effect of $T\sin(\theta/2)$. The combination of low tension and small wrap angle will yield the highest average impact forces. This effect is amplified for increasing tape speeds.

6 Discussion

Tape edge contact is a significant problem in achieving track densities beyond 40 tracks/mm (1000 tracks per inch (tpi)). Impacts between tape and roller or guide flanges induce LTM in the 1–2 KHz frequency range in the tape path. This is the frequency range beyond the bandwidth of the head servo actuator, i.e., the servo system is incapable of following such high frequency lateral vibrations of the tape, which can lead to track misregistration.

As tape manufacturers tend to use thinner tape to increase the volumetric storage density of a tape cartridge, the problem of tape edge contact might manifest itself more. It was observed that lower nominal tape tensions result in increasingly more severe tape flange impacts. Thinner tape requires the use of a lower tension to keep the stress in the tape constant. Hence, thinner tape might yield more severe tape edge contact. This conclusion is in agreement with Eq. (4). If the tape becomes thinner, the moment of inertia I decreases and the effective stiffness constant in the simulation becomes smaller, resulting in more severe impact.

Higher storage densities also imply higher data transfer rates. Thus, higher tape speeds will be necessary in future tape drive designs. Hence, LTM originated from tape flange contact will gain in importance since we found out that increased tape speed will increase the average magnitude of the tape flange impact drastically.

7 Conclusion

From our investigation it can be concluded that:

(1) Acoustic emission is a useful technique to monitor and characterize tape edge contact.
(2) Tape edge contact induces undesirable high frequency lateral tape motion, predominantly in the 1–2 kHz region.
(3) The maximum impact force between the flange of a roller and a tape edge was observed to occur for a half full tape reel. The magnitude of the impact force increases for increasing tape speed and decreases for increasing tension. The magnitude of the impact force decreases for increasing wrap angles.
(4) Although the one-dimensional "impact oscillator" model simplifies the tape flange contact problem drastically, it predicts the influence of operating and design parameters on tape/flange impact well.

References

[1] Taylor, R. J., Strahle, P., Stahl, J., and Talke, F. E., 2000, "Measurement of Cross-Track Motion of Magnetic Tapes," J. Inf. Storage Process. Syst., **2**, pp. 255–261.
[2] Childers, E. R., Imaino, W., Eaton, J. H., Jaquette, G. A., Koeppe, P. V., and Hellman, D. J., 2003, "Six Orders of Magnitude in Linear Tape Technology: The One-Terabyte Project," IBM J. Res. Dev., **47**(4), pp. 471–482.
[3] Lakshmikumaran, A. V., and Wickert, J. A., 1998, "Edge Buckling of Imperfectly Guided Webs," ASME J. Vibr. Acoust., **120**, pp. 346–352.
[4] Wang, J. H., Taylor, R. J., and Talke, F. E., 2003, "Lateral Motion and Edge Wear of Magnetic Tapes," Tribol. Int., **36**, pp. 423–431.
[5] Doyle, J. F., 1987, "Determining the Contact Force During the Transverse Impact of Plates," Exp. Mech., **21**(1), pp. 68–72.
[6] Goldade, A. V., and Bhushan, B., 2004, "Tape Edge Study in a Linear Tape

Drive with Single-Flanged Guides," J. Magn. Magn. Mater., **271**, pp. 409–430.
[7] Goldade, A. V., and Bhushan, B., 2003, "Measurement and Origin of Tape Edge Damage in a Linear Tape Drive," Tribol. Lett., **14**(3), pp. 167–180.
[8] Bhushan, B., Hinteregger, H. F., and Rogers, A. E. E., 1994, "Thermal Considerations for the Edge Guiding of Thin Magnetic Tape in a Longitudinal Tape Transport," Wear, **171**, pp. 179–193.
[9] Taylor, R. J., and Talke, F. E., 2005, "High Frequency Lateral Tape Motion and the Dynamics of Tape Edge Contact," Microsyst. Technol., **11**, pp. 1166–1170.
[10] Yan, T., and Jones, B. E., 2000, "Traceability of Acoustic Emission Measurements Using Energy Calibration Methods," Meas. Sci. Technol., **11**, pp. L9–L12.
[11] Clough, R. B., 1987, "The Energetics of Acoustic Emission Source Characterization," Mater. Eval., **45**, pp. 556–563.
[12] Hsu, N. N., and Breckenridge, F. R., 1981, "Characterization and Calibration of Acoustic Emission Sensors," Mater. Eval., **39**, pp. 60–68.
[13] Knigge, B., and Talke, F. E., 2000, "Contact Measurement Using Acoustic Emission Analysis and System Identification Methods," Tribol. Int., **33**, pp. 639–646.
[14] Matsumoto, M., Iida, A., and Hamaguchi, T., 1993, "Measurement of Slider/Disk Collision Forces Using Acoustic Emission Source Wave Analysis," Tribol. Trans., **36**(4), pp. 736–740.
[15] Senator, M., 1970, "Existence and Stability of Periodic Motions of a Harmonically Forced Impacting System," J. Acoust. Soc. Am., **47**(5) (part 2), pp. 1390–1397.
[16] Shaw, S. W., and Holmes, P. J., 1983, "A Periodically Forced Piecewise Linear Oscillator," J. Sound Vib., **90**(1), pp. 129–155.
[17] Brach, R. M., 1991, *Mechanical Impact Dynamics—Rigid Body Collisions*, Wiley, New York.
[18] Popov, E. G., 1999, *Engineering Mechanics of Solids*, Prentice-Hall, Englewood Cliffs, NJ.
[19] Broese van Groenou, A., 1991, "Tribology of Magnetic Storage Systems a Short Review," J. Magn. Magn. Mater., **95**, pp. 289–312.
[20] Raeymaekers, B., Etsion, I., and Talke, F. E., 2007, "The Influence of Operating and Design Parameters on the Magnetic Tape/Guide Friction Coefficient," Tribol. Lett., **25**(2), pp. 161–171.